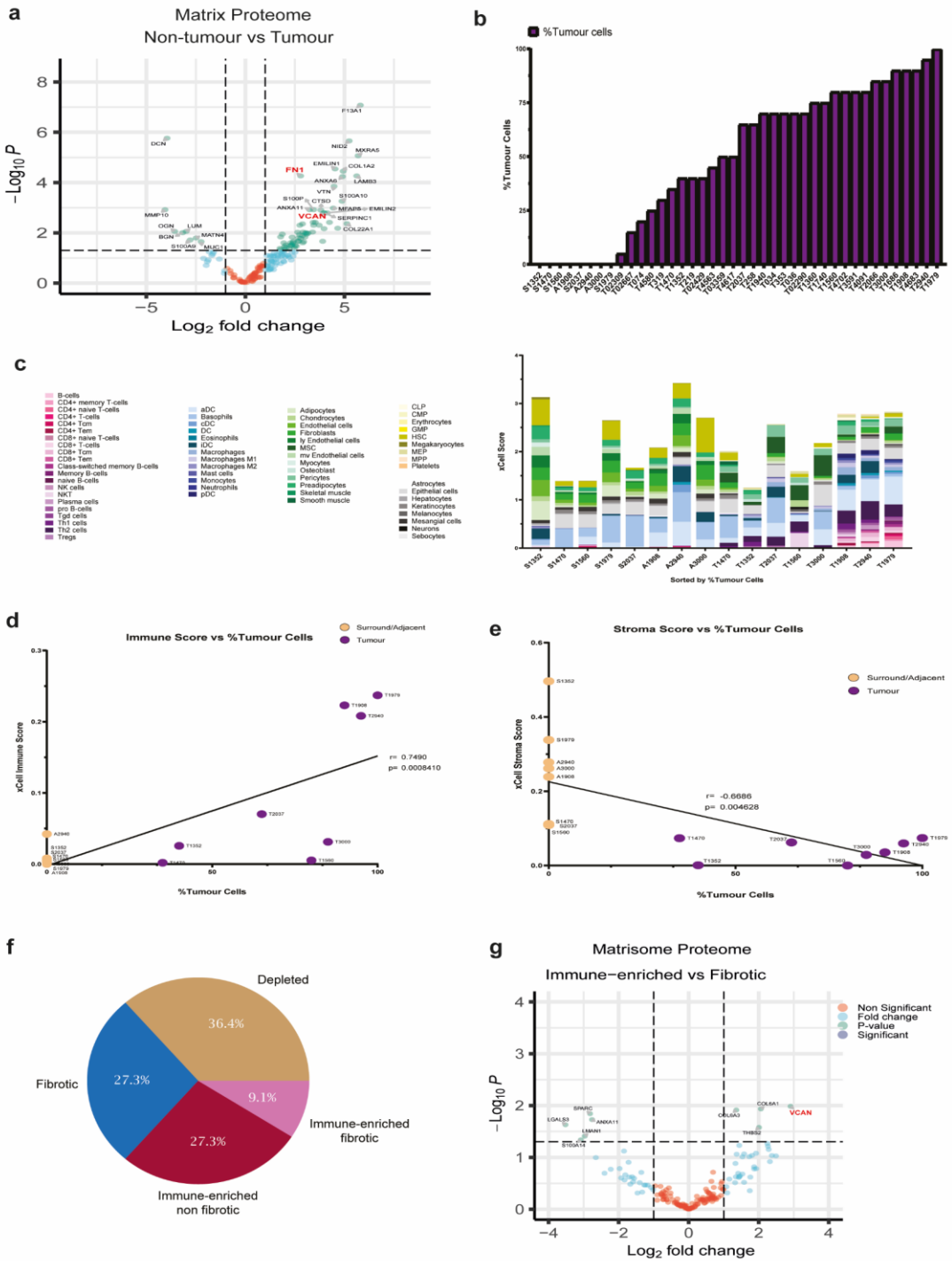

***Extended Data Figure 1* | Proteomics and tissue profiling of matched non-tumour and tumour patient tissues.**

(a), Volcano plot highlighting the significant differentially expressed matrisome proteins of matched non-tumour versus tumour tissues based on proteomics (n = 8). Genes of interest are coloured in red. **(b)**, Percentage of tumour cells in each matched non-tumour and tumour tissues (n=40) established by a pathologist on H&E staining. **(c)**, Individual cell composition of each matched non-tumour and tumour tissues based on xCell transcriptomic signatures[32] (n=8). **(d)**, Simple linear regression of the xCell immune score calculated by summing all the immune cell signatures with the percentage of tumour cells (n=8). **(e)**, Simple linear regression of the xCell stroma score calculated by summing all the stroma cell signatures with the percentage of tumour cells (n=8). Values for the Pearson correlation coefficient, r and the p-value, p are given on the graphs. **(f)**, Immune phenotype distribution of patient tumours based on signatures[30] (n = 32). **(g)**, Volcano plot highlighting the significantly differentially expressed matrisome proteins of immune-enriched (n = 8) versus fibrotic (n = 9) tumours based on proteomics. Genes of interest are coloured in red.

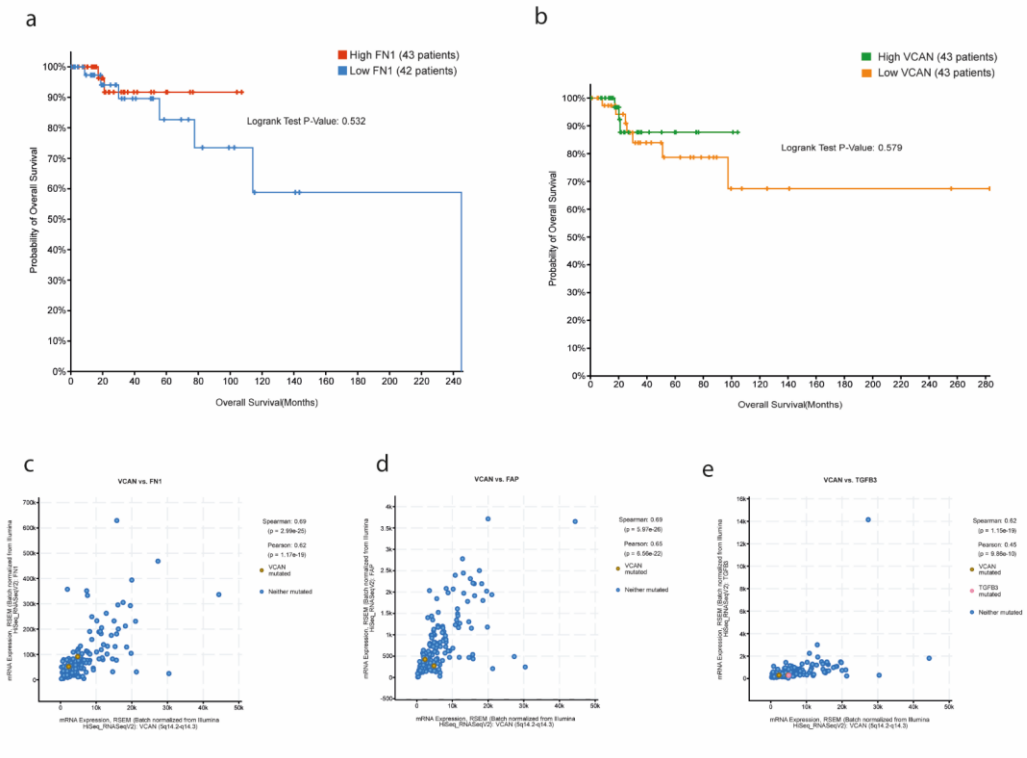

***Extended Data Figure 2* | Survival benefits of low FN1 and VCAN expression in the TCGA BRCA cohort for patients with breast cancer basal subtype.**

In the Cancer Genome Atlas Breast Invasive Carcinoma (TCGA-BRCA) data collection, the basal subtype gathers patients with triple-negative breast cancers (n=171). **(a)**, Survival Kaplan-Meier curve between high and low transcriptomic *FN1* expression in the TCGA BRCA Basal dataset. **(b)**, Survival Kaplan-Meier curve between high and low transcriptomic *VCAN* expression in the TCGA BRCA Basal dataset. **(c)**, Simple linear regression of the mRNA expression of *VCAN* compared to *FN1* in TCGA BRCA patients. **(d)**, Simple linear regression of the mRNA expression of *VCAN* compared to *FAP* in TCGA BRCA patients. **(e)**, Simple linear regression of the mRNA expression of *VCAN* compared to *TGFβ3* in TCGA BRCA patients.

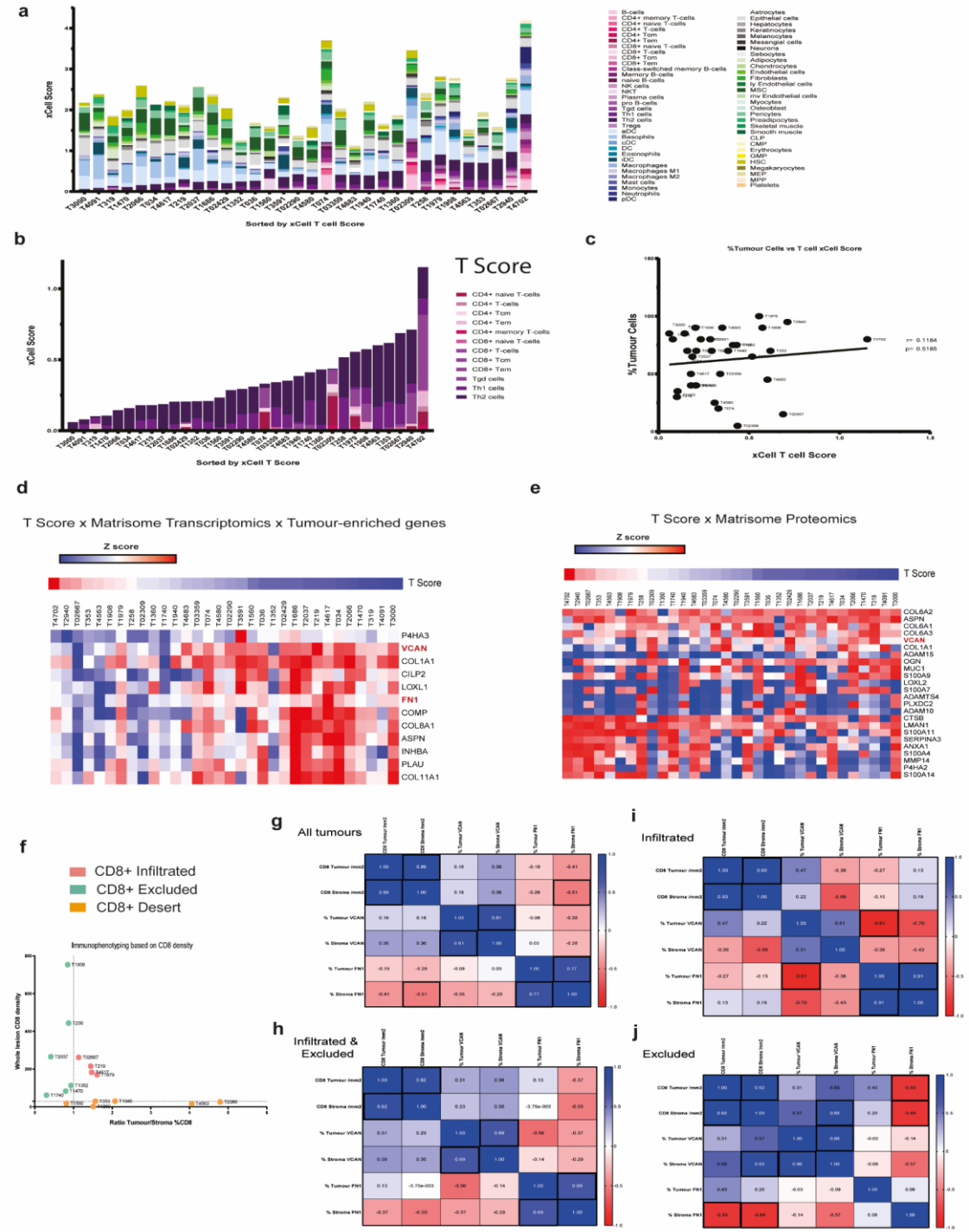

Extended Data Figure 3 | Correlation of T cells and matrisome composition in patient tumours by transcriptomics, proteomics and tissue staining.

(a), xCell transcriptomic signatures for 64 cell types on patient-derived tumours sorted by T-cell signatures[32] (n=32). **(b)**, Implementation of the T Score calculated by summing all the T-cell-related xCell transcriptomic signatures, excepting the Treg, in the whole patient tissues cohort (n=32). **(c)**, Simple linear regression of the percentage of tumour cells with T score. Values for the Pearson correlation coefficient, r and the p-value, p are given on the graphs (n=32). **(d)**, Heatmap showing the Pearson correlation of the tumour-enriched ECM genes that significantly correlate with T Score in each patient tumour sorted by decreasing xCell T Score on transcriptomes (n=32). 215 ECM genes were found correlating with T Score, only 12 of them were also found significantly enriched in tumours compared to non-tumour tissues. **(e)**, Heatmap showing the Pearson correlation of tumour-enriched ECM proteins that significantly correlate with T Score in each patient tumour sorted by decreasing xCell T Score on matrisomes (n=32). Only VCAN was also found significantly enriched in tumours compared to non-tumour tissues. **(f)**, Ratio of tumour/stroma CD8+ T-cell densities compared to whole lesion CD8+ density in tumours defining the infiltrated (ratio >1), excluded (ratio < 1) and desert phenotypes (n=16). **(g, h, i, j)**, Pearson correlation matrix of tumour and stromal CD8+ T-cell density, FN1 and VCAN coverage for **(g)**, all tumours (n=16), **(h)**, infiltrated and excluded tumours (n=10), **(i)**, infiltrated (n=4) and **(j)**, excluded tumours (n=6). Values of the Pearson correlation coefficients are given on the tables.

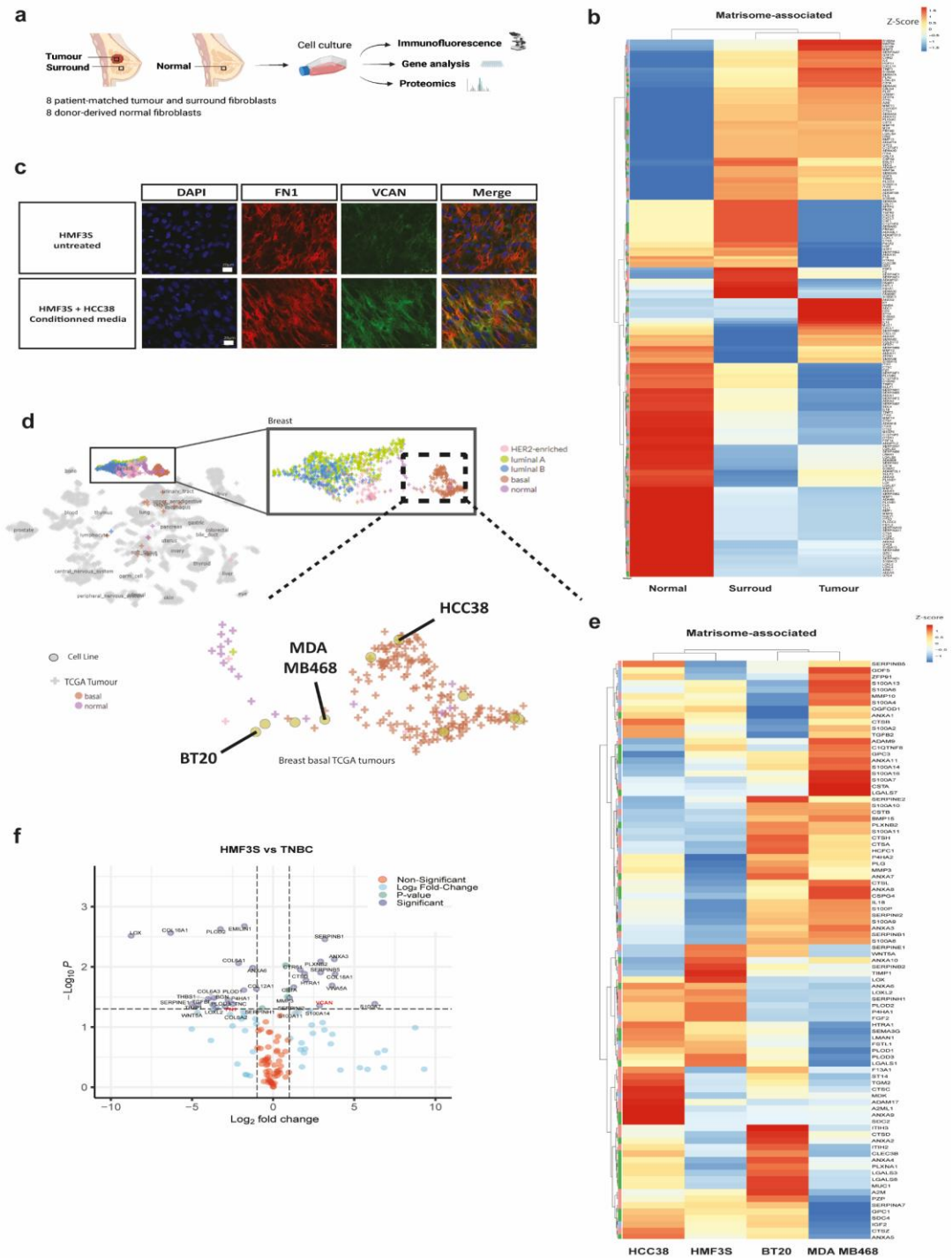

Extended Data Figure 4 | Patient-derived fibroblast, human triple-negative-breast cancer and fibroblast cell line matrisome profiling.

(a), Schematic of patient-derived fibroblast isolation and processing. **(b)**, Heatmap of the matrisome-associated protein relative expression of patient-derived fibroblasts in mass ratio. Red represents a protein enrichment and blue represents a protein depletion. **(c)**, Representatives images of DAPI, FN1 and VCAN immunofluorescent staining of untreated, TGFβ3-pretreated and HCC38-conditonned media pre-treated HMF3S fibroblasts cell line (n=3). **(d)**, (top) UMAP 2D projection aligning tumour and cell line expression data sorted by cancer lineage with a specific highlight on breast cancers. Dots are coloured by breast cancer subtypes. (bottom) Alignment of BT20, MDA MB468 and HCC38 cell lines with TCGA breast cancer tumours based on gene expression data. Cell lines are represented by a dot and patient TCGA tumour by a cross. Similarity of cell lines to tumour samples were evaluated by Pearson correlation distance between each cell line and tumour by DepMap Cellligner[35]. **(e)**, Heatmap of the matrisome-associated protein relative expression of human TNBC and fibroblast HMF3S cell lines in mass ratio. Red represents a protein enrichment and blue represents a protein depletion. **(f)**, Volcano plot showing statistical significance (P-value) versus magnitude of change (Fold-Change) of TNBC compared to fibroblast HMF3S cell lines. Significant upregulated proteins in each cell line condition were listed on the graphs.

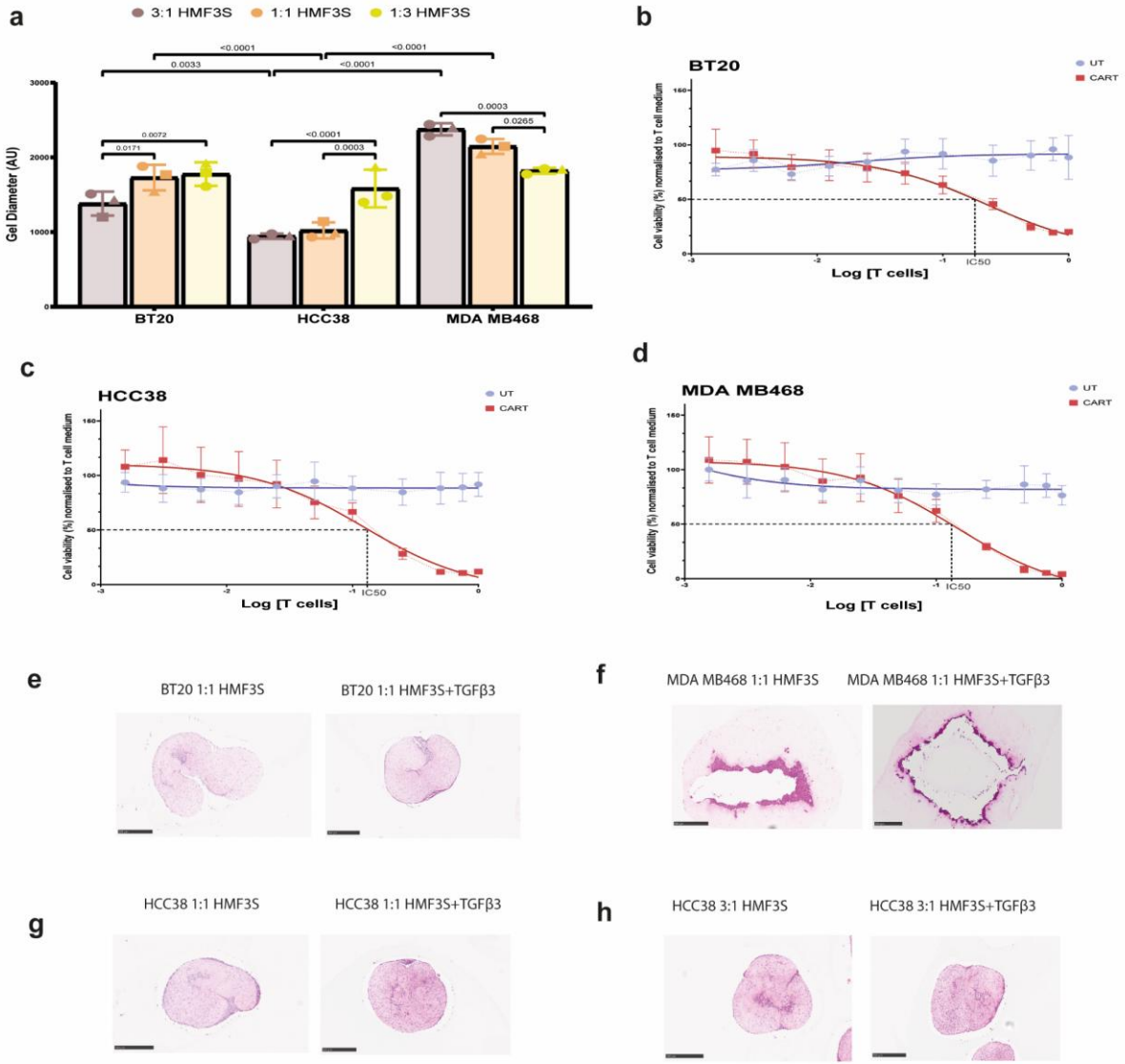

Extended Data Figure 5 | CAR T cytotoxicity assay in 3D in vitro TME models.

(a), Gel diameter measurement of 3D *in vitro* collagen gels seeded with cancer cell lines co-cultured with different ratios, 3:1, 1:1 and 1:3 to HMF3S fibroblasts. **(b-d)**, Percentage of cell viability of cell lines cultured in 2D and incubated with different ratios of UT and CAR T compared to T-cell medium (n=3), of **(b)**, BT20, **(c)**, HCC38, **(d)**, MDA MB468. IC50 represents the ratio of CAR T inhibiting 50% of the cell viability. **(e-h)**, Representative images of hematoxylin and eosin staining of 3D *in vitro* collagen gels of **(e)**, BT20 co-cultured in 1:1 ratio with untreated and TGFβ3-pre-treated HMF3S fibroblasts. **(f)**, MDA MB468 co-cultured in 1:1 ratio with untreated and TGFβ3-pre-treated HMF3S fibroblasts. **(g)**, HCC38 co-cultured in 1:1 ratio with untreated and TGFβ3-pre-treated HMF3S fibroblasts. **(h)**, HCC38 co-cultured in 3:1 ratio with untreated and TGFβ3-pre-treated HMF3S fibroblasts. Scale bar indicated 500μm.

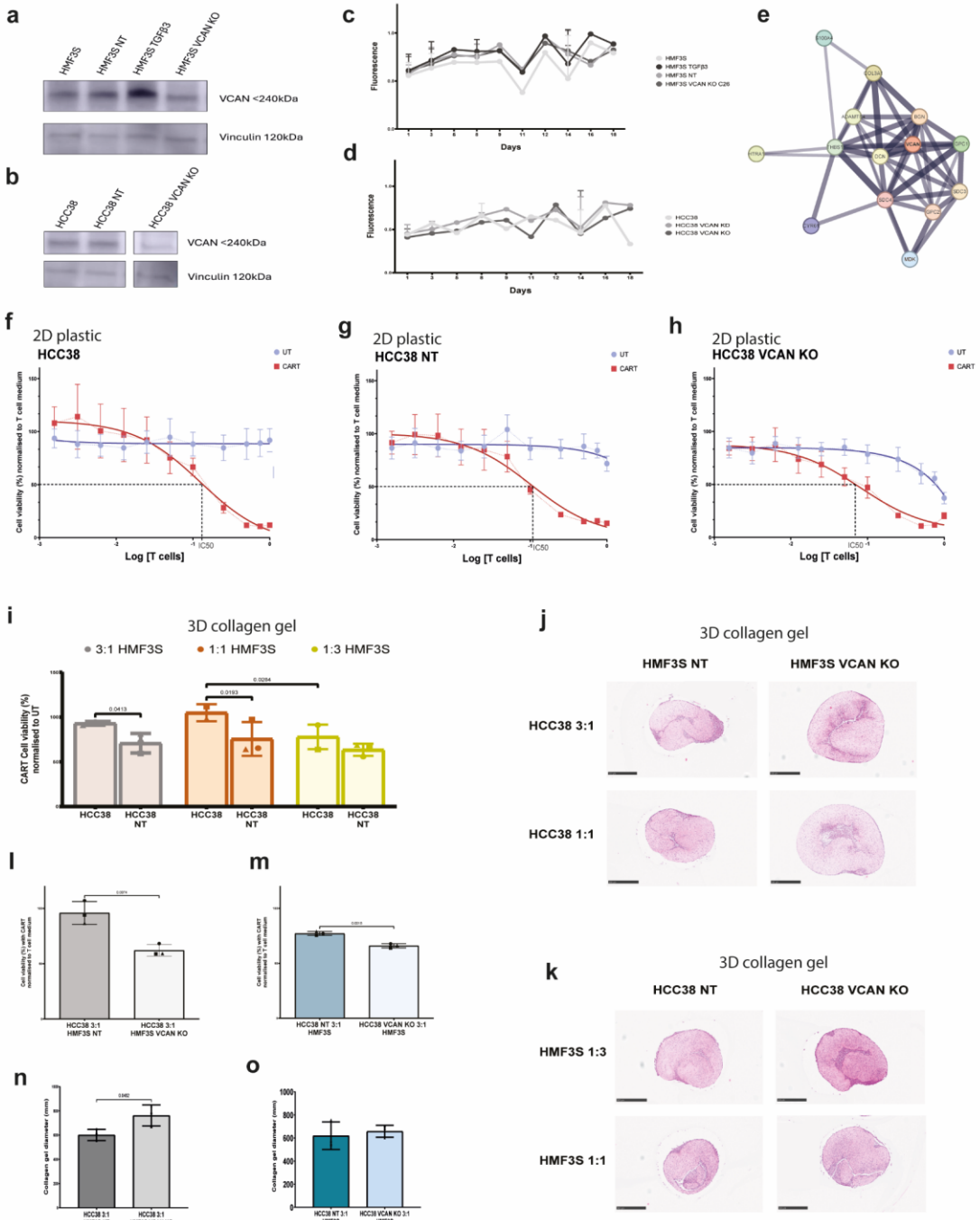

***Extended Data Figure 6* | CRISPR VCAN editing and *CAR T cytotoxicity assays in HMF3S and HCC38 3D in vitro TMEs*.**

(a,b), Western Immunoblotting against VCAN G1 domain (70kDa) and Vinculin (120kDa) in unedited and CRISPR-edited cell lines, **(a)**, for HMF3S and **(b)**, for HCC38. **(c,d)**, Cell viability assay over time in unedited and CRISPR-edited cell lines, **(c)**, for HMF3S and **(d)**, for HCC38 (n=3). **(e)**, STRING protein interaction network of VCAN. Nodes represent proteins and edges represent protein-protein associations known as interactions from curated databases and experimentally determined. **(f-h)**, Percentage of cell viability after incubation with different ratios of UT and CAR T compared to T-cell medium of HCC38 cancer cell lines cultured in 2D plastic. **(f)**, for HCC38, **(g)**, for HCC38 NT, and for **(h)**, for HCC38 VCAN KO (n=3 donors). **(i)**, Percentage of cell viability after incubation with CAR T compared to T-cell medium of HCC38 and HCC38 NT in 3D collagen gels with different ratios 3:1, 1:1, 1:3 of HMF3S. HCC38 NT showed increased sensitivity to CAR T-cell killing compared to HCC38 and will be used as a CRISPR-edition control. **(j,k)**, Hematoxylin and eosin staining of co-cultures of HCC38 cancer and HMF3S fibroblasT-cell lines seeded in different ratios 3:1, 1:1, 1:3 in 3D collagen gels before incubation with CAR T cells. **(l,m)**, Percentage of cell viability of co-cultures of HCC38 in 3:1 ratio to HMF3S in 3D collagen gels and incubated with CAR T cells compared to T-cell medium **(l)**, for HMF3S NT and VCAN KO and **(m)**, for HCC38 NT and VCAN KO. **(n,o)**, Collagen gel diameter (mm) of 3D *in vitro* TMEs with **(n)**, for HMF3S NT and VCAN KO and **(o)**, for HCC38 NT and VCAN KO. Each shape represents a T-cell donor (n=3, Student's t-test). NT= non-targeting.

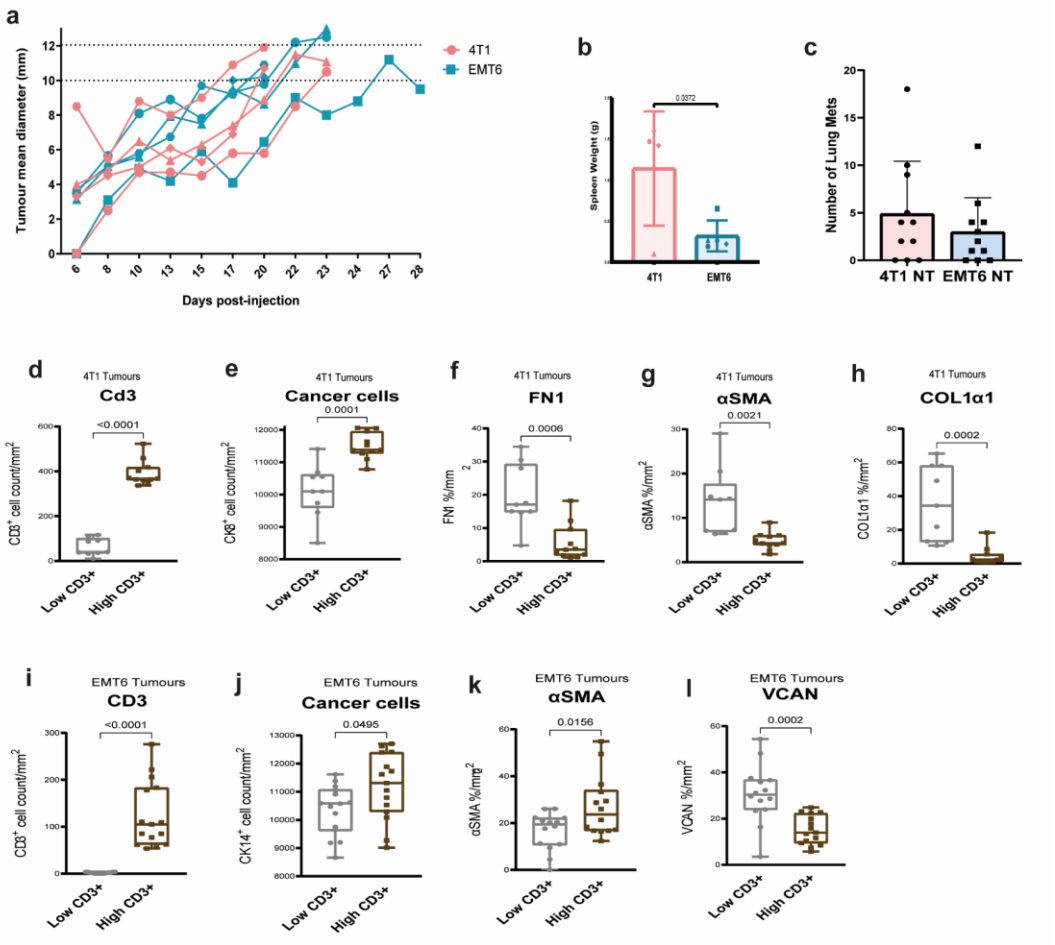

***Extended Data Figure 7* | 4T1 and EMT6 tumour growth and staining.**

(a), Tumour growth of 4T1 and EMT6 tumours for each mouse in mm over days. **(b)**, Spleen weight in g of mice bearing 4T1 and EMT6 tumours (n=4 for 4T1 and n=5 for EMT6, Student's T-test). **(c)**, Number of lung metastases (n=10 for 4T1 and n=10 for EMT6, Student's T-test). **(d-h)**, Quantification of immunohistochemical staining in areas with high CD3+ compared to low CD3+ cells in 4T1 tumours for **(d)**, CD3+ cell count per mm^2. **(e)**, CK8+ cell count per mm^2. **(f)**, FN1 coverage percentage per mm^2. **(g)**, αSMA coverage percentage per mm^2. **(h)**, COL1α1 coverage percentage per mm^2. **(i-l)**, Quantification of immunohistochemical staining in areas with high CD3 compared to low CD3+ cells in EMT6 tumours for **(i)**, CD3+ cell count per mm^2. **(j)**, CK14+ cell count per mm^2. **(k)**, αSMA coverage percentage per mm^2. **(l)**, VCAN coverage percentage per mm^2 (Student's T-test).

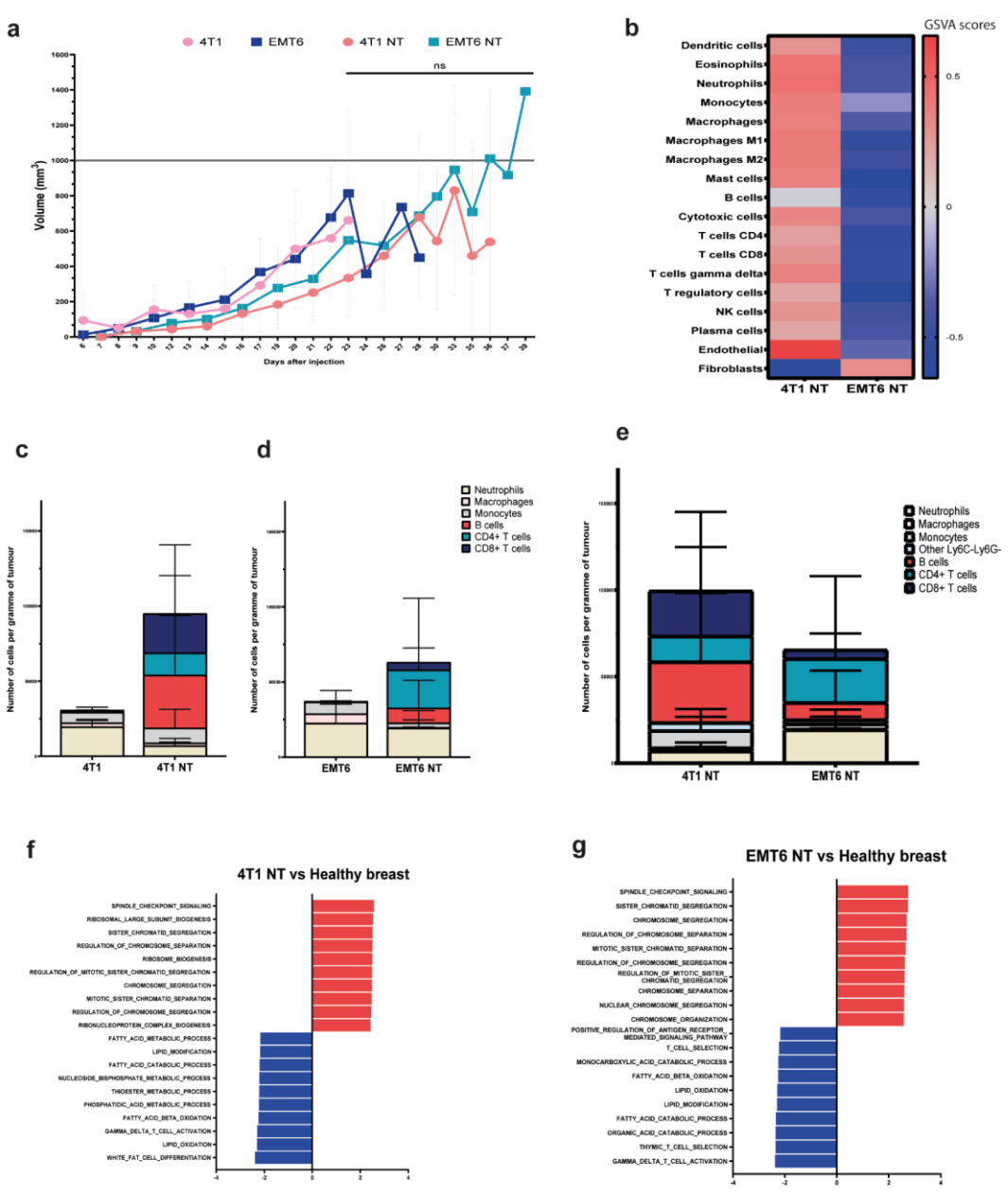

***Extended Data Figure 8* | Tumour growth and immune cell composition of 4T1 NT and EMT6 NT compared to 4T1 and EMT6.**

(a), Tumour growth of 4T1 NT and EMT6 NT tumours compared to 4T1 and EMT6 tumours in volume in mm^3 over days (n=5 for 4T1 NT, n=6 for EMT6 NT, n=4 for 4T1 and n=5 for EMT6, Multiple paired T-test, ns indicate a p-value ≥ 0.05). **(b)**, Heatmap of Consensus TME signatures for 18 cell types for 4T1 NT and EMT6 NT tumours based on transcriptomics. **(c-e)**, Number of live CD45+ immune cells isolated /g of tumour from **(c)**, 4T1 and 4T1 NT tumours. **(d)**, EMT6 and EMT6 NT tumours. **(e)**, 4T1 NT and EMT6 NT tumours (n=2 for 4T1, n=5 for 4T1 NT, n=5 for EMT6, n=6 for EMT6 NT). **(f-g)**, Bar plot of the top positive and negative hallmark pathways ranked by normalised enrichment scores from GSEA on transcriptomics from **(f)**, 4T1 NT tumours compared to healthy murine mammary fat pad tissues. **(g)**, EMT6 NT tumours compared to healthy murine mammary fat pad tissues (n=5 for 4T1 NT, n=6 for EMT6 NT, n=2 for healthy mammary tissues). NT= non-targeting.

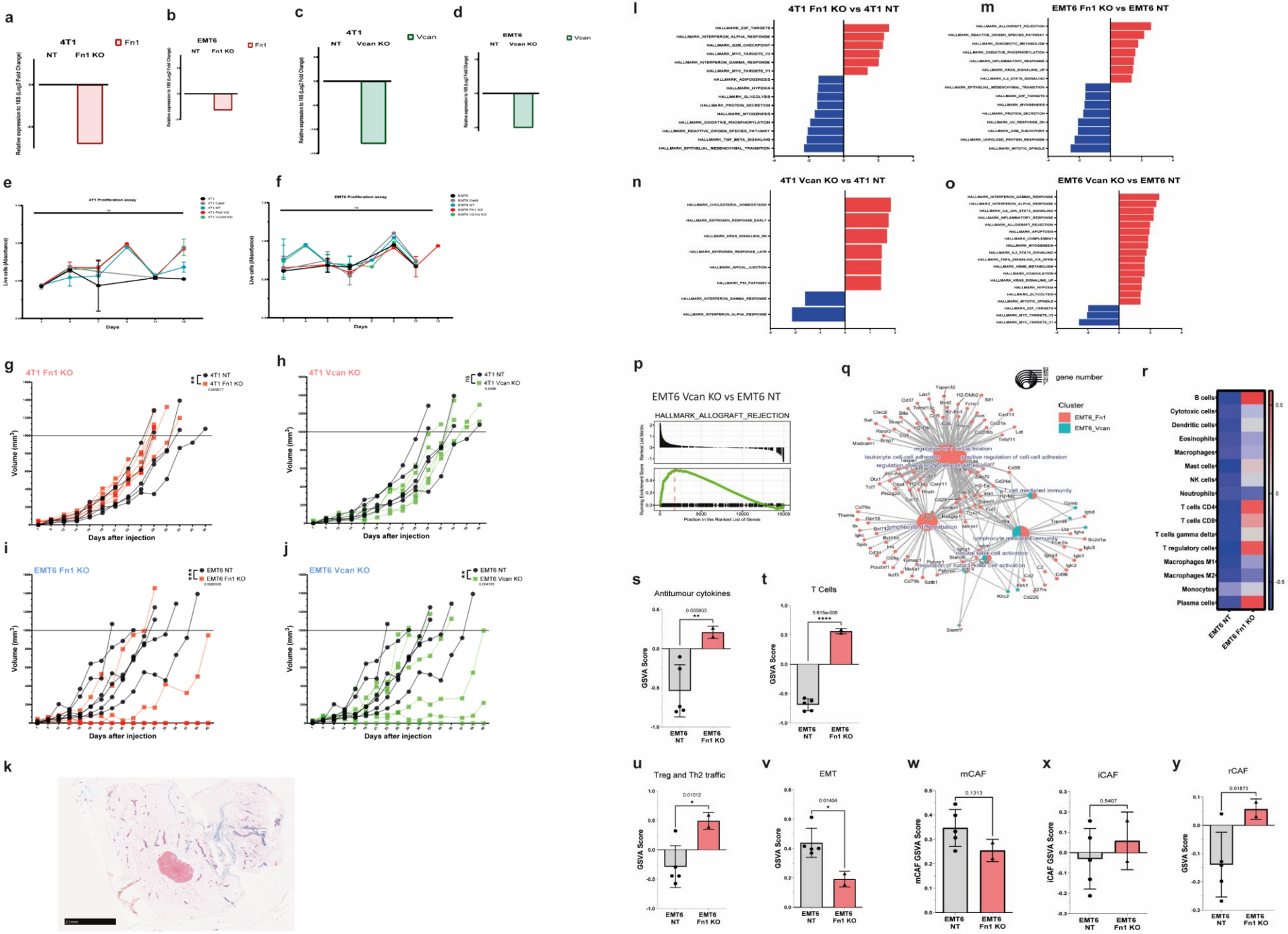

***Extended Data Figure 9* | *Fn1* and *Vcan* KO in 4T1 and EMT6 tumours.**

(a, b, c, d), Quantification of *Fn1* and *Vcan* expression by qPCR on the cell lines **(a)**, 4T1 NT and *Fn1* KO. **(b)**, EMT6 NT and *Fn1* KO. **(c)**, 4T1 NT and *Vcan* KO. **(d)**, EMT6 NT and *Vcan* KO. **(e, f)**, Cell viability assay over time of the cell lines **(e)**, 4T1, 4T1 Cas9, 4T1 NT, 4T1 *Fn1* KO and 4T1 *Vcan* KO. **(f)**, EMT6, EMT6 Cas9, EMT6 NT, EMT6 *Fn1* KO and EMT6 *Vcan* KO (n=3). **(g,h,l,j)**, Tumour growth in volume in mm^3 over days of **(g)**, 4T1 NT and *Fn1* KO. **(h)**, 4T1 NT and *Vcan* KO. **(i)**, EMT6 NT and *Fn1* KO. **(j)**, EMT6 NT and *Vcan* KO. **(k)**, Image of a EMT6 *Fn1* KO tumour after complete tumour regression. **(l,m,n,o)**, Bar plot of the top positive and negative hallmark pathways ranked by normalised enrichment scores on **(l)**, 4T1 *Fn1* KO compared to 4T1 NT. **(m)**, EMT6 *Fn1* KO compared to EMT6 NT **(n)**, 4T1 *Vcan* KO compared to 4T1 NT. **(o)**, EMT6 *Vcan* KO compared to EMT6 NT. **(p)**, Enrichment plots for genes involved in the allograft rejection hallmark in EMT6 *Vcan* KO compared to EMT6 NT tumours. **(q)**, GSEA network plot of enriched genes from EMT6 *Fn1* KO (in pink) and EMT6 *Vcan* KO (in green) tumours compared to EMT6 NT. **(r)**, Heatmap of the Consensus TME cell types involved in the Immune score for EMT6 NT and EMT6 *Fn1* KO. **(s, t, u, v,w,x,y)**, GSVA enrichment score in EMT6 NT and *Fn1* KO lines **(s)**, for antitumour cytokines signature. **(t)**, for T cells signature. **(u)**, for Treg and Th2 traffic signature. **(v)**, for EMT signature. **(w)**, for mCAF signature. **(x)**, for inflammatory CAF signature. **(y)**, for rCAF signature. (n=5 for 4T1 NT, n=6 for 4T1 Fn1 KO, n=5 for 4T1 Vcan KO, n=6 for EMT6 NT, n=2 for EMT6 Fn1 KO, n=5 for EMT6 Vcan KO, n=2 for healthy mammary fat pad, Multiple paired t-tests)

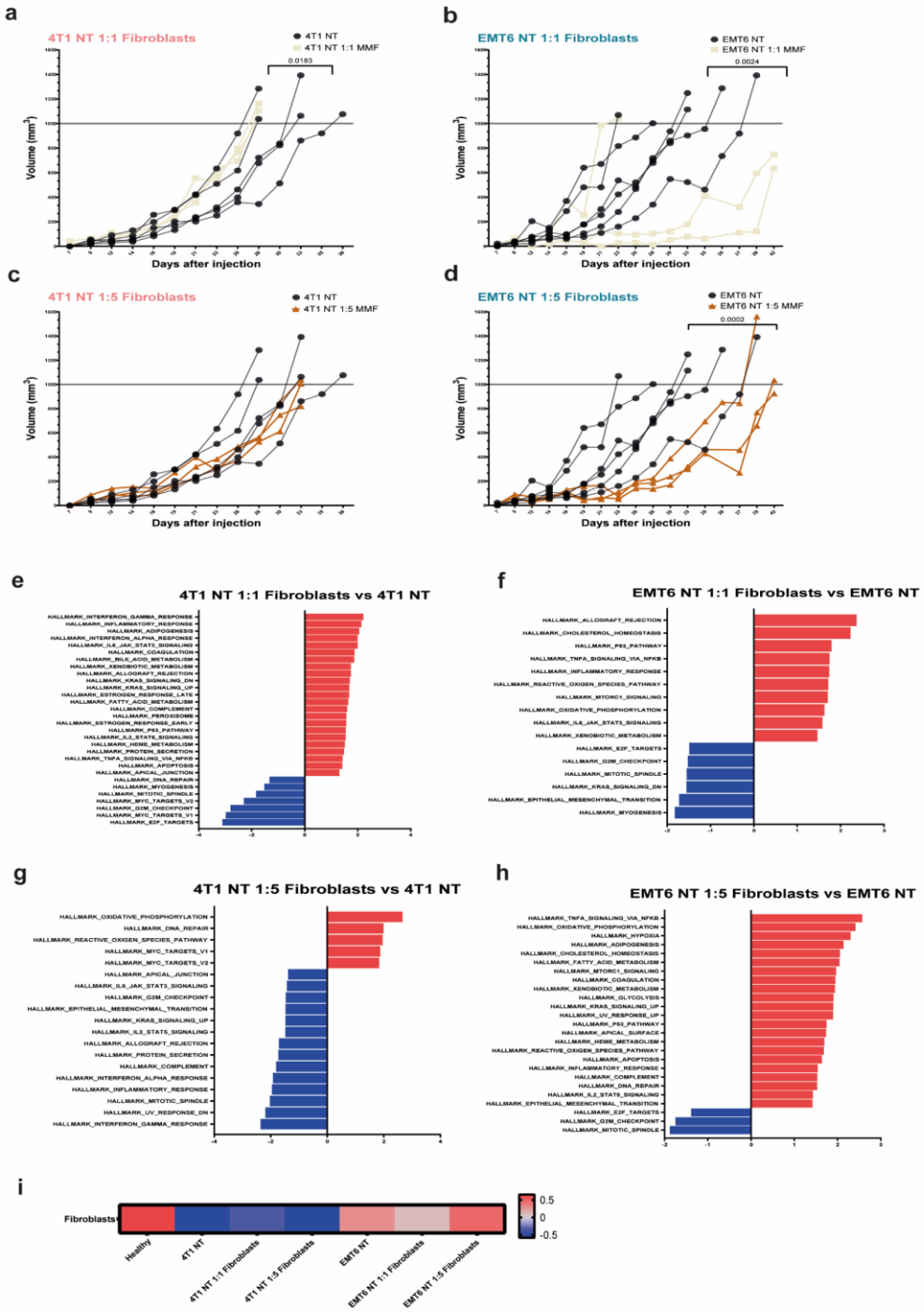

***Extended Data Figure 10* | Co-injection of healthy fibroblasts in 4T1 and EMT6 tumours.**

(a, b, c, d), Tumour growth in volume in mm^3 over days for similar number of cancer cells of **(a)**, 4T1 NT and MMF in 1:1 ratio. **(b)**, EMT6 NT and MMF in 1:1 ratio. **(c)**, 4T1 NT and MMF in 1:5 ratio. **(d)**, EMT6 NT and MMF in 1:5 ratio. **(e, f, g, h)**, Bar plot of the top positive and negative hallmark pathways ranked by normalised enrichment scores for **(e)**, 4T1 NT 1:1 MMF compared to 4T1 NT. **(f)**, EMT6 NT 1:1 MMF compared to EMT6 NT. **(g)**, 4T1 NT 1:5 MMF compared to 4T1 NT. **(h)**, EMT6 NT 1:5 MMF compared to EMT6 NT. **(i)**, Heatmap of the Consensus TME fibroblast signature. (n=5 for 4T1 NT, n=3 for 4T1 NT 1:1 Fibroblasts, n=3 for 4T1 NT 1:5 Fibroblasts, n=6 for EMT6 NT, n=3 for EMT6 NT 1:1 Fibroblasts, n=3 for EMT6 NT 1:5 Fibroblasts. Multiple paired T-test).

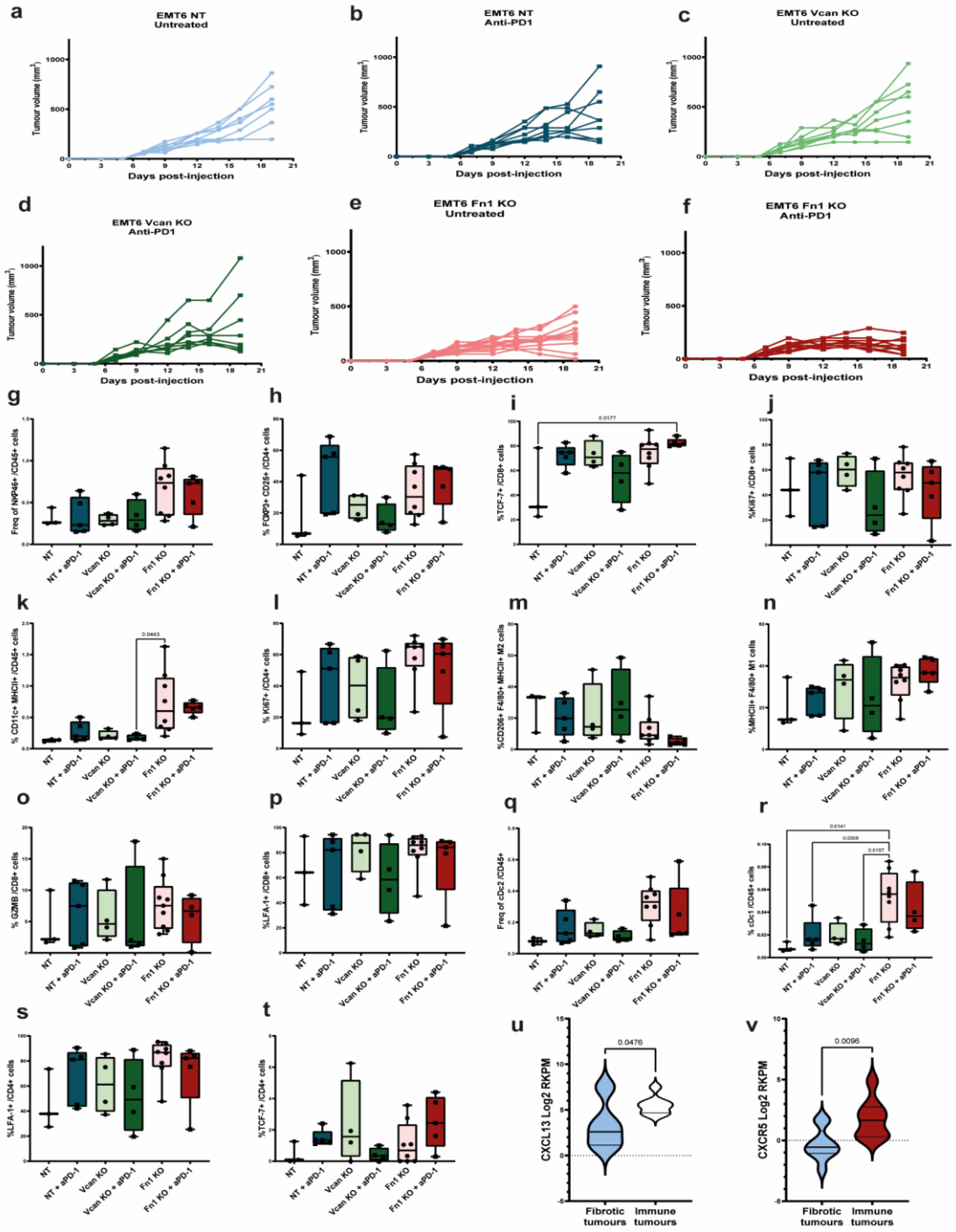

Extended Data Figure 11* | CRISPR KO and *CAR T-cell viability assays.

(a-f), Tumour growth in volume in mm^3 over days of **(a)**, Untreated-EMT6 NT. **(b)**, anti-PD1-treated EMT6 NT. **(c)**, Untreated-EMT6 *Vcan* KO. **(d)**, anti-PD1-treated EMT6 *Vcan* KO. **(e)**, Untreated-EMT6 *Fn1* KO. **(f)**, anti-PD1-treated EMT6 *Fn1* KO. **(g-t),** Quantification per gram of tumours of EMT6 NT, anti-PD1-treated EMT6 NT, EMT6 *Vcan* KO, anti-PD1-treated EMT6 *Vcan* KO, EMT6 *Fn1* KO, anti-PD1-treated EMT6 *Fn1* KO of **(g)**, NKP46+ CD45+ live cells in tumours. **(h)**, FOXP3+CD25+ CD4+ live cells in tumours. **(i)**, TCF7+ CD8+ live cells in tumours. **(j)**, Ki67+ CD8+ live cells in tumours. **(k)**, MHCII+ CD11c+ CD45+ live cells. **(l)**, Ki67+ CD4+ live cells in tumours. **(m)**, CD206+ F4/80+ MHCII+ live cells in tumours. **(n)**, CD206- F4/80+ MHCII+ live cells in tumours. **(o)**, GZMB+ CD8+ live cells in tumours. **(p)**, LFA1+ CD8+ live cells in tumours. **(p)**, XCR1- CD11c+ CD45+ live cells in tumours. **(r)**, XCR1+ CD11c+ CD45+ live cells in tumours. **(s)**, LFA1+ Cd4+ live cells in tumours. **(t)**, TCF7+ CD4+ live cells in tumours. **(u)**, CXCL3 expression in patient tumour transcriptomics. **(v)**, CXCR5 expression in patient tumour transcriptomics.